

RESEARCH ARTICLE

A specific type of insulin-like peptide regulates the conditional growth of a beetle weapon

Yasukazu Okada^{1*}, Masako Katsuki², Naoki Okamoto³, Haruna Fujioka^{1,4}, Kensuke Okada⁵

1 Department of Biological Sciences, Tokyo Metropolitan University, Hachioji, Tokyo, Japan, **2** Laboratory of Applied Entomology, Graduate School of Agricultural and Life Sciences, The University of Tokyo, Tokyo, Japan, **3** Department of Entomology, Institute for Integrative Genome Biology, University of California, Riverside, Riverside, California, United States of America, **4** Department of General Systems studies, Graduate School of Arts and Sciences, The University of Tokyo, Komaba, Tokyo, Japan, **5** Graduate School of Environmental and Life Science, Okayama University, Okayama, Japan

* okayasukazu@gmail.com



OPEN ACCESS

Citation: Okada Y, Katsuki M, Okamoto N, Fujioka H, Okada K (2019) A specific type of insulin-like peptide regulates the conditional growth of a beetle weapon. *PLoS Biol* 17(11): e3000541. <https://doi.org/10.1371/journal.pbio.3000541>

Academic Editor: Laurent Keller, University of Lausanne, SWITZERLAND

Received: March 18, 2019

Accepted: October 31, 2019

Published: November 27, 2019

Copyright: © 2019 Okada et al. This is an open access article distributed under the terms of the [Creative Commons Attribution License](https://creativecommons.org/licenses/by/4.0/), which permits unrestricted use, distribution, and reproduction in any medium, provided the original author and source are credited.

Data Availability Statement: The data supporting the findings of this study are available from figshare (DOI: [10.6084/m9.figshare.9734780](https://doi.org/10.6084/m9.figshare.9734780); <https://figshare.com/s/609486022a3df39169bf>).

Funding: Funding was received from JSPS Kakenhi 18H04815, 17H05938, 17K19381, and 19H04913 to YO and 18K0641700 to KO; (<https://www.jspss.go.jp/english/index.html>); Yamada Science Foundation to YO (<http://www.yamadazaidan.jp/english.html>); Postdoctoral Fellowship for Research Abroad from the JSPS to NO (<https://www.jspss.go.jp/english/e-pd/ab.htm>); Naito

Abstract

Evolutionarily conserved insulin/insulin-like growth factor (IGF) signaling (IIS) has been identified as a major physiological mechanism underlying the nutrient-dependent regulation of sexually selected weapon growth in animals. However, the molecular mechanisms that couple nutritional state with weapon growth remain largely unknown. Here, we show that one specific subtype of insulin-like peptide (ILP) responds to nutrient status and thereby regulates weapon size in the broad-horned flour beetle *Gnatocerus cornutus*. By using transcriptome information, we identified five *G. cornutus* ILP (*GcorILP1–5*) and two *G. cornutus* insulin-like receptor (*GcorInR1*, *-2*) genes in the *G. cornutus* genome. RNA interference (RNAi)-mediated gene silencing revealed that a certain subtype of ILP, *GcorILP2*, specifically regulated weapon size. Importantly, *GcorILP2* was highly and specifically expressed in the fat body in a condition-dependent manner. We further found that *GcorInR1* and *GcorInR2* are functionally redundant but that the latter is partially specialized for regulating weapon growth. These results strongly suggest that *GcorILP2* is an important component of the developmental mechanism that couples nutritional state to weapon growth in *G. cornutus*. We propose that the duplication and subsequent diversification of IIS genes played a pivotal role in the evolution of the complex growth regulation of secondary sexual traits.

Introduction

Sexual selection often leads animals to evolve strikingly exaggerated male ornaments and weapons [1], which are often characterized by heightened nutritional sensitivity during growth. Intraspecific variation of secondary sexual trait size is in turn often associated with condition-dependent mating tactics, such as fighting, sneaking, or dispersal [2–4]. Therefore, these traits are most exaggerated in the largest and best-conditioned individuals but rudimentary in low-conditioned males, commonly resulting in positive allometries of weapons and ornaments [5,6]. Such conditional expression of sexual traits is a good example of the adaptive

Foundation Subsidy for Dispatch of Young Researchers Abroad to NO (https://www.naito-f.or.jp/en/joseikn/jo_index.php?data=detail&grant_id=WAK). The funders had no role in study design, data collection and analysis, decision to publish, or preparation of the manuscript.

Competing interests: The authors have declared that no competing interests exist.

Abbreviations: AaILP3, *A. aegypti* ILP3; BIGFLP, IGF-like ILP in *Bombyx*; DILP, *Drosophila* ILP; dsGFP, double-stranded RNA for green fluorescent protein; dsRNA, double-stranded RNA; dsx, doublesex; EW, elytra width; GcorILP, *G. cornutus* ILP; GcorInR, *G. cornutus* InR; IGF, insulin-like growth factor; IIS, insulin/IGF signaling; ILP, insulin-like peptide; InR, insulin-like receptor; JH, juvenile hormone; KD, knockdown; ObILP2, *Ooceraea biroi* ILP2; PCA, principal component analysis; rel. exp., relative expression; RNAi, RNA interference; TcILP, *T. castaneum* ILP; TcInR, *T. castaneum* InR.

evolution of phenotypic complexity [7]. Consequently, conditional growth is a fundamental mechanism underlying the evolution of exaggerated phenotypes and their complex development; however, an in-depth understanding of these mechanisms is lacking [8,9].

The major nutrient-dependent endocrine pathway, insulin/insulin-like growth factor (IGF) signaling (IIS), has been identified as a mechanism that can link exaggerated trait growth and nutritional condition [9–11]. In the Japanese rhinoceros beetle, *Trypoxylus dichotomus*, down-regulation of IIS by the knockdown (KD) of receptor gene (*InR*) caused a dramatic reduction in horn length in adults but resulted in only a slight reduction in wing and genital size [10]. In a dung beetle, *Onthophagus taurus*, KD of transcription factor *FOXO* but not *InR* affected horn length [12]. This ancient and conserved pathway that couples growth with available nutrients is considered to have been repeatedly co-opted in lineages that experienced strong sexual selection [10]. However, the deployed genes may be more diverse than previously expected.

The most upstream central players in IIS are insulin-like peptides (ILPs), which include insulin and IGFs in mammals [13] and multiple ILPs in insects [14,15]. In both mammals and insects, the production, secretion, and action of insulin/IGFs/ILPs are mainly regulated by the nutritional status [16–18]. They activate receptor tyrosine kinases (i.e., insulin receptor and IGF type-I receptor) in mammals and InRs in insects to accelerate cellular growth, proliferation, and metabolism [14,15,19,20].

Although this signal transduction mechanism is conserved across taxa, individual gene members of this pathway, especially ligands and receptors, may have undergone substantial diversification. For example, several insect species possess two or three InRs [14,21]. Interestingly, in the brown planthopper, two receptors alternately regulate the polyphenic development of short- and long-winged morphs [22]. Further, in the yellow fever mosquito and clonal raider ant, a certain type of ILP is known to regulate reproductive status [23–26]. Recent genome-wide investigations implied that insect ILPs are also highly diversified within and across species. Relatively basal clades, such as Orthoptera, possess only one ILP [27], whereas there are up to four ILPs in the red flour beetle [28], eight in the fruit fly and yellow fever mosquito [29,30], 10 in the pea aphid [31], and more than 40 in the silkworm [32]. In insects, ILP production and secretion from the brain are considered as the principal mechanisms for nutrient-dependent systemic growth and metabolism [14,15,18]. However, other non-neurosecretory ILPs also have important growth functions in specific stages and/or tissues [15,33–35].

Given that gene-duplications play pivotal roles in the evolution of phenotypic complexity [36,37], the frequent multiplications of insect ILPs and InRs suggest the potential for functional diversification, such as trait- and stage-specific functions. So far, however, whether and how different types of ILPs and InRs functionally contribute to phenotypic complexity remain largely unknown. Here, we focused on the developmental plasticity of a beetle weapon and tested the hypothesis that specific types of IIS ligands and receptors regulate weapon growth.

Males of the broad-horned flour beetle *G. cornutus* have exaggerated mandibles used in male–male combat (Fig 1), and males possessing larger mandibles have an advantage in these contests [38]. Large males have disproportionately larger mandibles (i.e., positive allometry), and this variation is mostly generated by the amount and quality of larval diet [38,39]. Therefore, the male mandibles of *G. cornutus* are a good model for the heightened conditional growth of a secondary sexual trait. Here, using *G. cornutus*, we investigated the molecular basis of this conditional growth by identifying the specific peptides that link nutritional condition with weapon growth.

Broad-horned flour beetle larvae were cultured in groups (approximately $n = 200$) for 30–60 days in whole-wheat flour medium. This high-density culture condition inhibits the pupation of larvae, but the isolation from the culture immediately induces pupation. The beginning

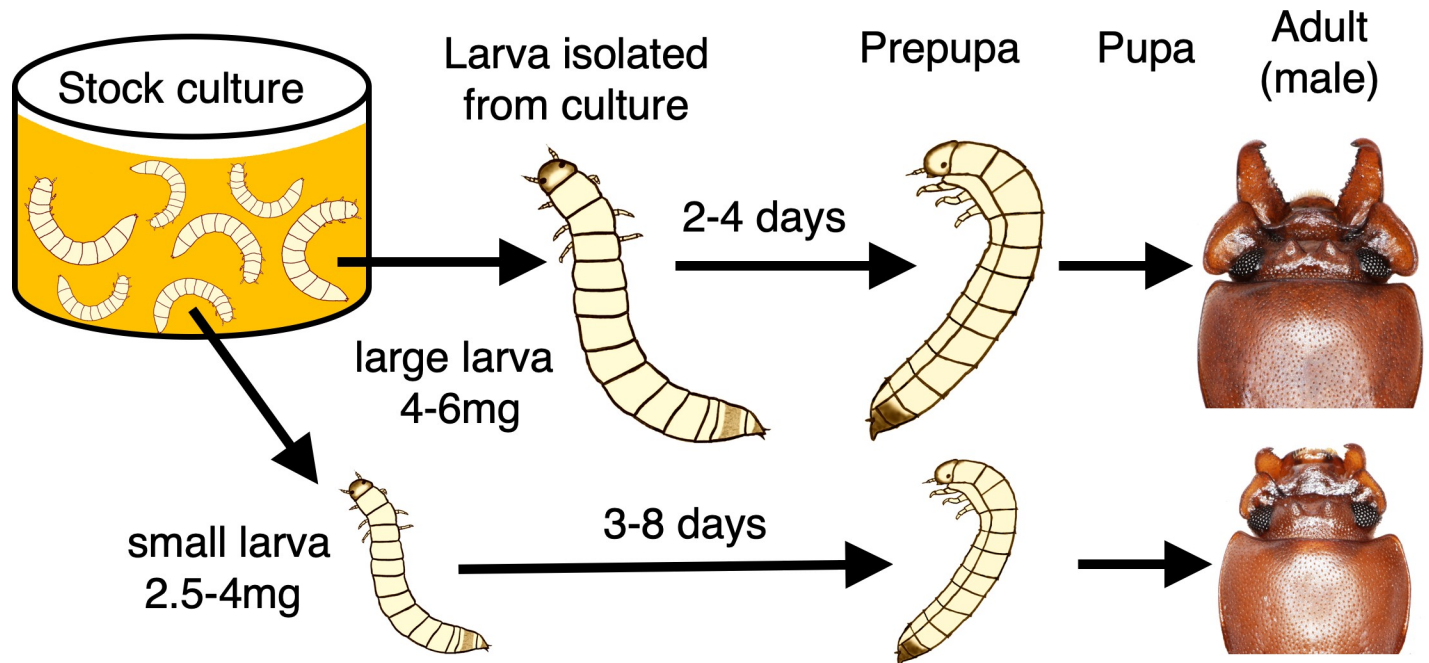


Fig 1. Development of *G. cornutus* and experimental procedure.

<https://doi.org/10.1371/journal.pbio.3000541.g001>

of pupation is visually detectable by the characteristic L-shape of prepupa. For prepupation, large individuals (>4 mg) take 2–4 days, whereas small individuals (2.5–4 mg) take 3–8 days. See details in [S1 Fig](#) and [Materials and Methods](#).

Results

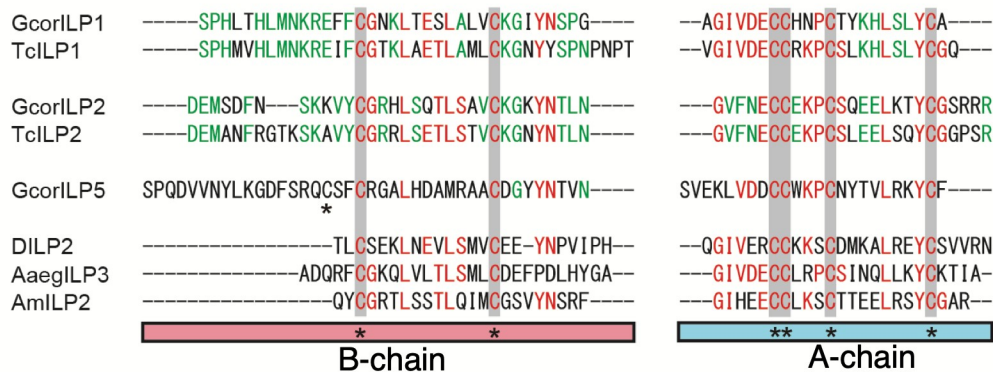
The schedule of metamorphic development in *G. cornutus*

Prior to molecular developmental analyses, we determined the detailed patterns of development and its condition dependence in *G. cornutus*. Unsurprisingly, larval size variation originated from the amount of dietary intake before metamorphosis, and the nutritional condition eventually determines the male sexual phenotype in this species ([Fig 1](#)). In *G. cornutus*, the timing of pupation is determined by a “critical size” and food availability, similar to many other holometabolous insects [40]. From the preliminary experiment, larvae (30–60 days from egg oviposition) weighing 2.5–4 mg were defined as poorly fed “small individuals,” and those weighing >4 mg were defined as sufficiently fed “large individuals” ([Fig 1](#), [S1 Fig](#), also see [Materials and Methods](#)). Note that smaller larvae take longer for prepupation ([Fig 1](#), [S1 Fig](#)). This negative relationship between larval weight and the time required for prepupation implies that small, low-conditioned larvae do not pupate immediately. Consequently, the developmental process slightly differed between large and small individuals in the following gene expression analyses.

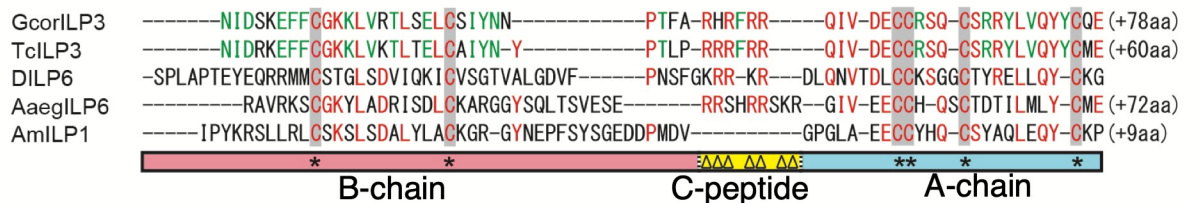
Identification and classification of ILPs and InRs in *G. cornutus*

The genome of the red flour beetle *Tribolium castaneum* contains four *ILP* (*TcILP1–4*) and two *InR* (*TcInR1* and *TcInR2*) genes [28,41]. Using *TcILP* and *TcInR* sequences as queries, *G. cornutus* *ILP* and *InR* candidates were retrieved by local BLASTx against the larval transcriptome [42].

A Insulin-like peptides



B IGF-like peptides



C DILP7-like peptides



Fig 2. Predicted mature structures of insulin-like, IGF-like, and DILP7-like peptides in *G. cornutus*. Domain-based alignments of (A) insulin-like peptides, (B) IGF-like peptides, and (C) DILP7-like peptides from the broad-horned flour beetle (*G. cornutus*), red flour beetle (*T. castaneum*), fruit fly (*Drosophila melanogaster*), yellow fever mosquito (*Aedes aegypti*), and honey bee (*Apis mellifera*). Representative ILPs of the fruit fly (DILP2, -6, -7), mosquito (AaegILP3, -5, -6), and honey bee (AmILP1, -2) are shown. Highly conserved amino acid residues between all ILPs are shown in red, and those between orthologous ILPs in *G. cornutus* and *T. castaneum* are shown in green. Asterisks below the alignment denote conserved Cys residues. Note that signal peptide and C-peptide of insulin-like ILP are omitted to show the mature heterodimeric peptides. For the complete structure, see S6 Fig. AaegILP, *A. aegypti* ILP; AmILP, *A. mellifera* ILP; DILP, *Drosophila* ILP; GcorILP, *G. cornutus* ILP; IGF, insulin-like growth factor; ILP, insulin-like peptide; TcILP, *T. castaneum* ILP.

<https://doi.org/10.1371/journal.pbio.3000541.g002>

We identified five *ILP* genes in the *G. cornutus* transcript (Fig 2, S2 Fig, S1 Material). The amino acid phylogeny showed that four of the five *GcorILP* sequences had close similarity to the four *TcILPs*, indicating the clear orthologous relationships of these four genes (S3 Fig). We named these four ILP genes *GcorILP1*, -2, -3, and -4 according to the nomenclature of *T. castaneum* [28]. The fifth ILP gene, which is novel in *G. cornutus*, was named *GcorILP5*. Although cross-species orthologs (ILP1–4) were clustered, only terminal nodes were supported by high bootstrap values; thus, evolutionary relationships among different orthologs were unclear (S3 Fig).

Since ILPs are highly diverged in their amino acid sequences except for some critical residues necessary for appropriate processing and tertiary structure, phylogeny-based analyses are often insufficient [34], and our data fit such a pattern. Therefore, based on domain structures

and characteristic cysteine residues [18], we manually aligned and elucidated three ILP subtypes (Fig 2, S2 Fig) [18,28,43]: insulin-like peptides that contain long C-peptides with two dibasic cleavage sites at the boundary with the B- and A-chain (GcorILP1, GcorILP2, and GcorILP5; Fig 2A); IGF-like peptides that contain relatively short C-peptides, which usually lack a dibasic cleavage site at the boundary with the B- and/or A-domain (GcorILP3; Fig 2B); and *Drosophila* ILP (DILP) 7-like peptides that are highly conserved across insect lineages (GcorILP4; Fig 2C). Note that mature structures after the removal of C-peptides are shown in Fig 2 for readability (see S2 Fig for full propeptide structure).

For receptors, we identified two *InRs* in *G. cornutus* transcripts. Construction of the protein phylogeny revealed that these two *GcorInRs* had clear orthologs in the *T. castaneum* genome (S4 Fig), and thus, they were named *GcorInR1* and *GcorInR2*.

Condition-dependent expression of *GcorILP2* during development

To profile the developmental expression pattern of *GcorILPs*, we quantified the whole-body transcript levels from larval to pupal stages in the two different classes of conditioned samples: large and small individuals (preparation details in Fig 1 and Materials and Methods). The results revealed that *GcorILP2* had a clear peak in day-2 larvae (immediately before prepupation) only in the large individuals (Fig 3B). Notably, *GcorILP2* levels were constantly low in small larvae. Even if we consider that small larvae take longer for pupation (Fig 1, S1 Fig), there is no apparent peak during the course of metamorphic, postfeeding development in small larvae.

The increase in *GcorILP3* was also observed in day-2 larvae and the prepupal stage of large individuals; however, small larvae also exhibited a similar increase in *GcorILP3* around the prepupal stage (day-6 larvae and day-0 and day-1 prepupae; Fig 3C). These results indicate that IGF-like *GcorILP3* is maintained at low levels during larval stages but increases during metamorphosis, irrespective of larval size. This result is consistent with the dominant expression of IGF-like peptides during metamorphosis in *Bombyx* and *Drosophila* [33–35]. We did not find clear positive nutritional responses of other *ILPs* (*GcorILP1*, *GcorILP4*, and *GcorILP5*), although they were slightly heightened in day-0 larvae (Fig 3A, 3D and 3E). These results suggest that, among the five *GcorILPs*, the expression of *GcorILP2* was specifically positively correlated with nutritional condition during postfeeding metamorphic development.

Sex and tissue specificities of *GcorILP2*: Condition-dependent expression in fat body

To further demonstrate the positive relationships between nutritional condition and *GcorILP2* expression, we additionally examined the conditional expression of *GcorILP2* in day-2 larvae with larval sexing and weighing. We found that there were significant positive relationships between larval weight and *GcorILP2* levels in both males and females (Fig 4A).

To determine the production source of *GcorILPs*, tissue-specific expression of *GcorILPs* was analyzed by qPCR using dissected brain, fat body, and gut tissues, which are the major sources of insect *ILPs* [18,44], in day-2 larvae. In insects, the principal *ILP*-producing cells that are tightly associated with nutrient-dependent growth and metabolism regulation are considered to be the neurosecretory cells in the brain [15]. The IGF-like *ILPs* in *Drosophila* (DILP6) and *Bombyx* (BIGFLP) are mainly produced in the fat body [33–35], and DILP7 is produced in neurons of abdominal ganglia [45,46]. Consistent with this, insulin-like *GcorILP1*, *GcorILP5*, and Dilp7-like *GcorILP4* were predominantly expressed in the brain but did not exhibit heightened expression in large larvae (S5 Fig).

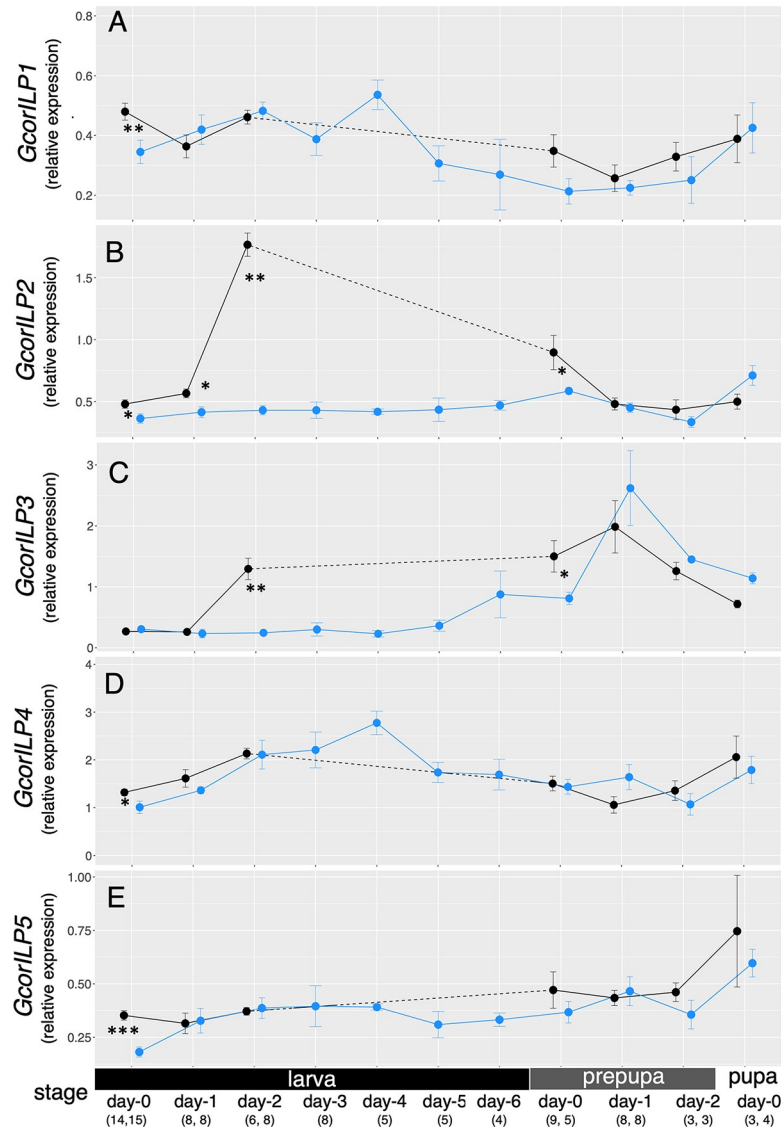


Fig 3. Developmental dynamics of insulin-like peptide transcription. *GcorILP* expression levels relative to *Gcorgapdh* were quantified by qPCR for the whole body. Black: large larvae; blue: small larvae. Results are presented as mean \pm SE. Asterisks show significant differences between large and small larvae of the same stages (Mann-Whitney U test, * $p < 0.05$, ** $p < 0.01$, *** $p < 0.001$). Larvae day-0 to day-6 corresponds to the days after larval isolation from culture. Prepupae day-0, -1, -2, and pupae day-0 correspond to the days after prepupation and pupation. Since large larvae take fewer days for prepupation (see Fig 1, S1 Fig), there were no large 3–6-day larvae (dashed line). The number of replicates is shown in parentheses. The underlying data in this figure are available from figshare (DOI: [10.6084/m9.figshare.9734780](https://doi.org/10.6084/m9.figshare.9734780); <https://figshare.com/s/609486022a3df39169bf>). *Gcorgapdh*, *G. cornutus* glyceraldehyde 3-phosphate dehydrogenase; *GcorILP*, *G. cornutus* insulin-like peptide; qPCR, quantitative PCR.

<https://doi.org/10.1371/journal.pbio.3000541.g003>

IGF-like *GcorILP3* was ubiquitously expressed across tissues, and its expression was heightened in the gut of large larvae but not in other tissues (S5 Fig). Interestingly, one of the ILPs, *GcorILP2*, was specifically and highly expressed in the fat body, and this expression was more abundant in large larvae (Fig 4B). During dissection, we noticed that the body cavity of large larvae is almost filled with the fat body, whereas that of small larvae contained less fat body (approximately half of the body volume, personal observation by YO). Therefore, the whole-body differences in *GcorILP2* expression (Fig 3B) may be explained by both fat body activity

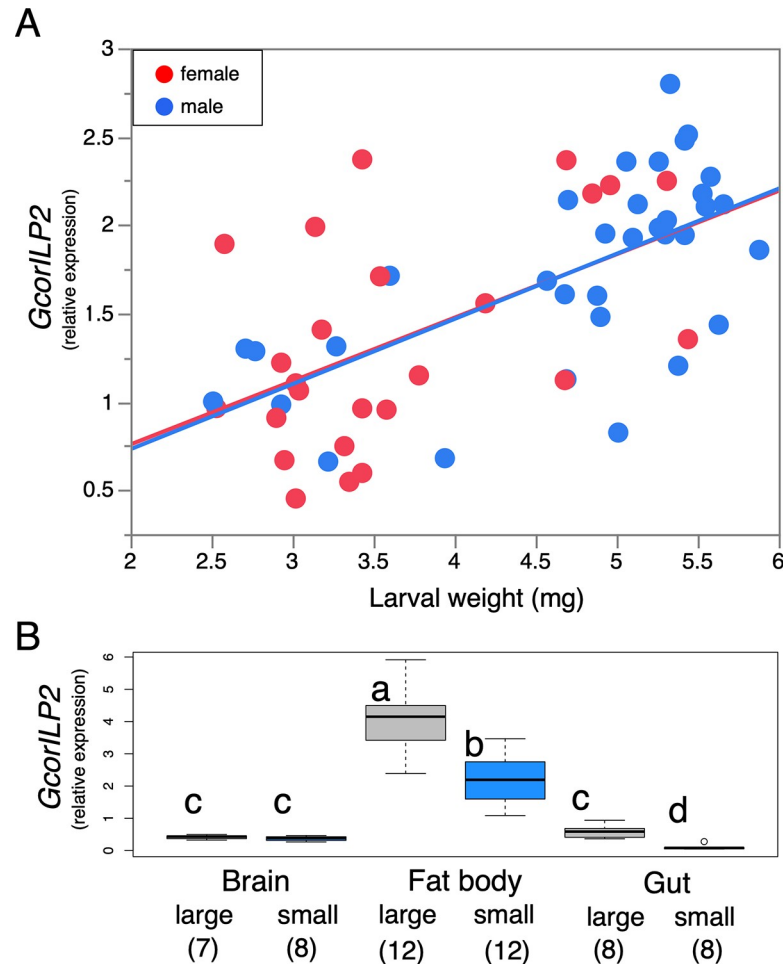


Fig 4. Levels of *GcorILP2* transcription in the fat body of larvae. (A) Both males (blue) and females (red) exhibited body size-dependent *ILP2* expression (regression analysis, female, $Y = 0.359X + 0.040$, $R^2 = 0.25$, $p = 0.01$; male, $Y = 0.369X - 0.006$, $R^2 = 0.42$, $p < 0.0001$). $n = 25$ and 34 for females and males, respectively. (B) *GcorILP2* was specific to the fat body and more abundant in large larvae. Different letters indicate significant differences (Steel-Dwass test). Gray (left): large; blue (right): small. Day-2 larvae were subjected to analysis. Gene expression levels relative to *Gcorgapdh* were quantified by qPCR. The underlying data in this figure are available from figshare (DOI: [10.6084/m9.figshare.9734780](https://doi.org/10.6084/m9.figshare.9734780); <https://figshare.com/s/609486022a3df39169bf>). *Gcorgapdh*, *G. cornutus* glyceraldehyde 3-phosphate dehydrogenase; *GcorILP2*, *G. cornutus* *ILP2*; *ILP2*, insulin-like peptide 2; qPCR, quantitative PCR.

<https://doi.org/10.1371/journal.pbio.3000541.g004>

and the relative amount of fat body per individual. The above stage- and tissue-specific expression analyses pose a hypothesis that the fat body-derived *GcorILP2* could be the best candidate for the molecular nature that regulates nutrient-dependent weapon growth in *G. cornutus*.

GcorILP2-coupled condition with weapon growth

RNA interference (RNAi)-driven gene KDs were conducted to test the developmental functions of five *GcorILPs* and two *GcorInRs* by double-stranded RNA (dsRNA) injection in the final instar larvae. dsRNA dosages were gradually titrated down from 50 ng to 0.1 ng (50 ng, 10 ng, 1 ng, 0.2 ng, and 0.1 ng) to find the highest dosages providing viable adults that allowed for phenotyping (dosages and KD efficiencies are summarized in [S1 Table](#)).

We found that silencing *GcorILP2* (45% transcript reduction, [S1 Table](#)) yielded a clear reduction in male mandible size ([Fig 5A and 5B](#)). In *GcorILP2*^{RNAi} males, a clear decline of

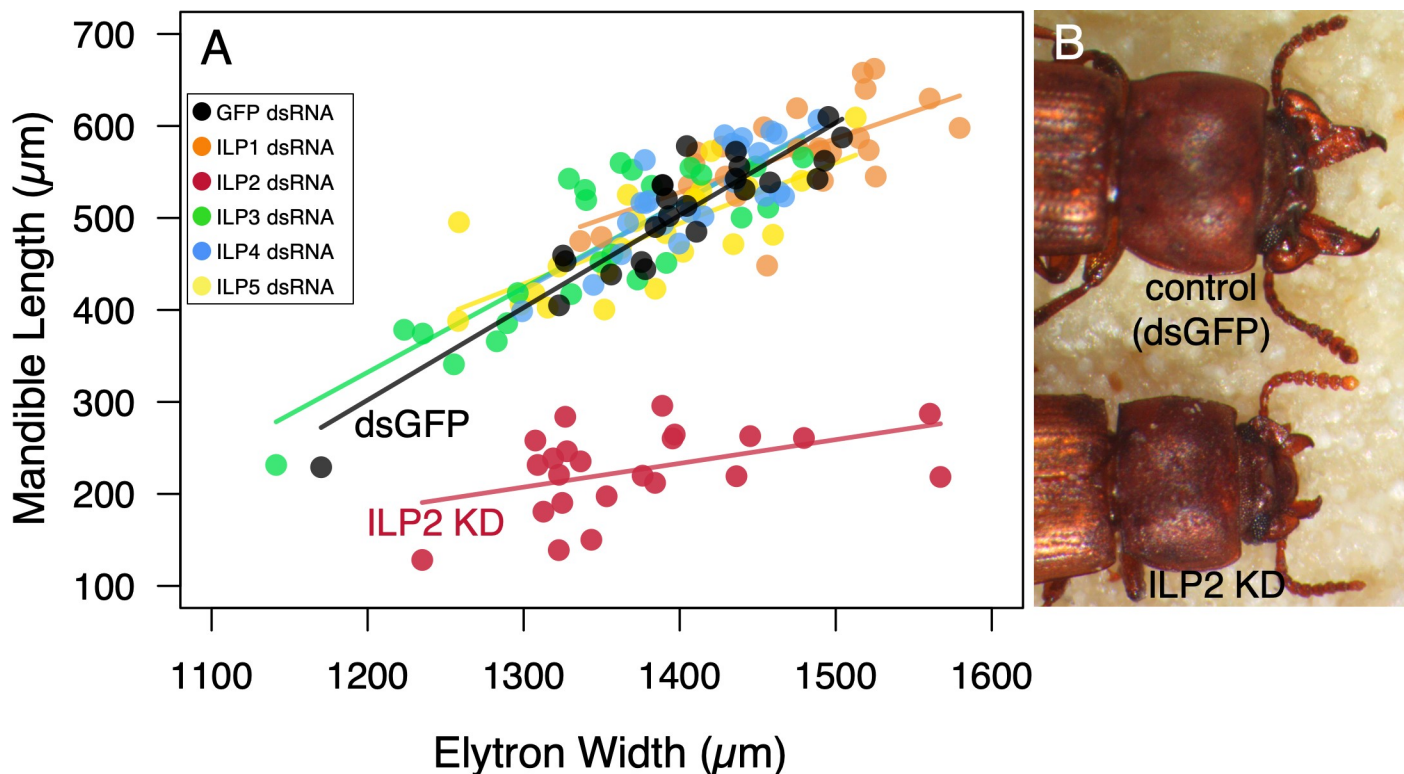


Fig 5. KD of a specific type of ILP (*GcorILP2*) diminishes conditional growth of male mandibles in *G. cornutus*. (A) KD phenotypes of 5 ILPs (*Gcor1-5*) shown as scatterplots of mandible length against body size (elytron width). Dots and regression lines of different treatments are shown by different colors. $n = 24, 23, 24, 24, 24$, and 24 for ds*Gcor1-5* and dsGFP, respectively. (B) *GcorILP2*^{RNAi} males had smaller mandible size than the control males had. Two males had similar elytra sizes but clearly different mandible sizes and moderately different head and prothorax sizes. The underlying data in this figure are available from figshare (DOI: [10.6084/m9.figshare.9734780](https://doi.org/10.6084/m9.figshare.9734780); <https://figshare.com/s/609486022a3df39169bf>). dsGFP, double-stranded RNA for GFP; dsRNA, double-stranded RNA; *GcorILP2*, *G. cornutus* ILP2; GFP, green fluorescent protein; ILP, insulin-like peptide; KD, knockdown; RNAi, RNA interference.

<https://doi.org/10.1371/journal.pbio.3000541.g005>

regression slope was detected compared to the control treatment (double-stranded RNA for green fluorescent protein [dsGFP]) (Fig 5A, ANCOVA [KD treatment as a factor, body size defined as elytra width {EW} as a covariate], body size \times treatment, $F = 26.1, p < 0.001$, Bonferroni correction, see S2 Table for full model statistics), implying that body size-dependent growth of mandibles was diminished in *GcorILP2*^{RNAi} males.

In contrast, interaction terms (treatment \times body size) were not significant in the other four *GcorILP* KDs (Fig 5A, ANCOVA, body size \times treatment, *GcorILP1*^{RNAi}, $F = 6.43, p = 0.089$; *GcorILP3*^{RNAi}, $F = 0.28, p = 1$; *GcorILP4*^{RNAi}, $F = 0.132, p = 1$; *GcorILP5*^{RNAi}, $F = 4.91, p = 1$, Bonferroni correction). In these cases, the interaction term (body size \times treatment) was removed from the statistical model. Consequently, the effects of KD treatments were not significant, indicating that regression intercepts were not altered by KDs of these ILPs (ANCOVA, treatment: *GcorILP1*^{RNAi}, $F = 0.346, p = 1$; *GcorILP3*^{RNAi}, $F = 1.45, p = 1$; *GcorILP4*^{RNAi}, $F = 1.71, p = 0.99$; *GcorILP5*^{RNAi}, $F = 0.25, p = 1$, see S2 Table for full model statistics).

Since *GcorILP* KDs are conducted at the highest levels (37%–85% reductions, S1 Table), morphogenetic effects of *GcorILP* KDs other than those of *GcorILP2* are negligible, at least at the prepupal stage. Additionally, log–log scale allometric analysis of mandible length against body size (defined as EW) showed that allometric coefficient α was > 1 in the control treatment ($\alpha = 3.37 \pm 0.65$ [95% CI]) but was not different from 1 in *GcorILP2*^{RNAi} males ($\alpha = 1.86 \pm 1.58$ [95% CI]), supporting the positive allometry in control males but not in *GcorILP2*^{RNAi} males.

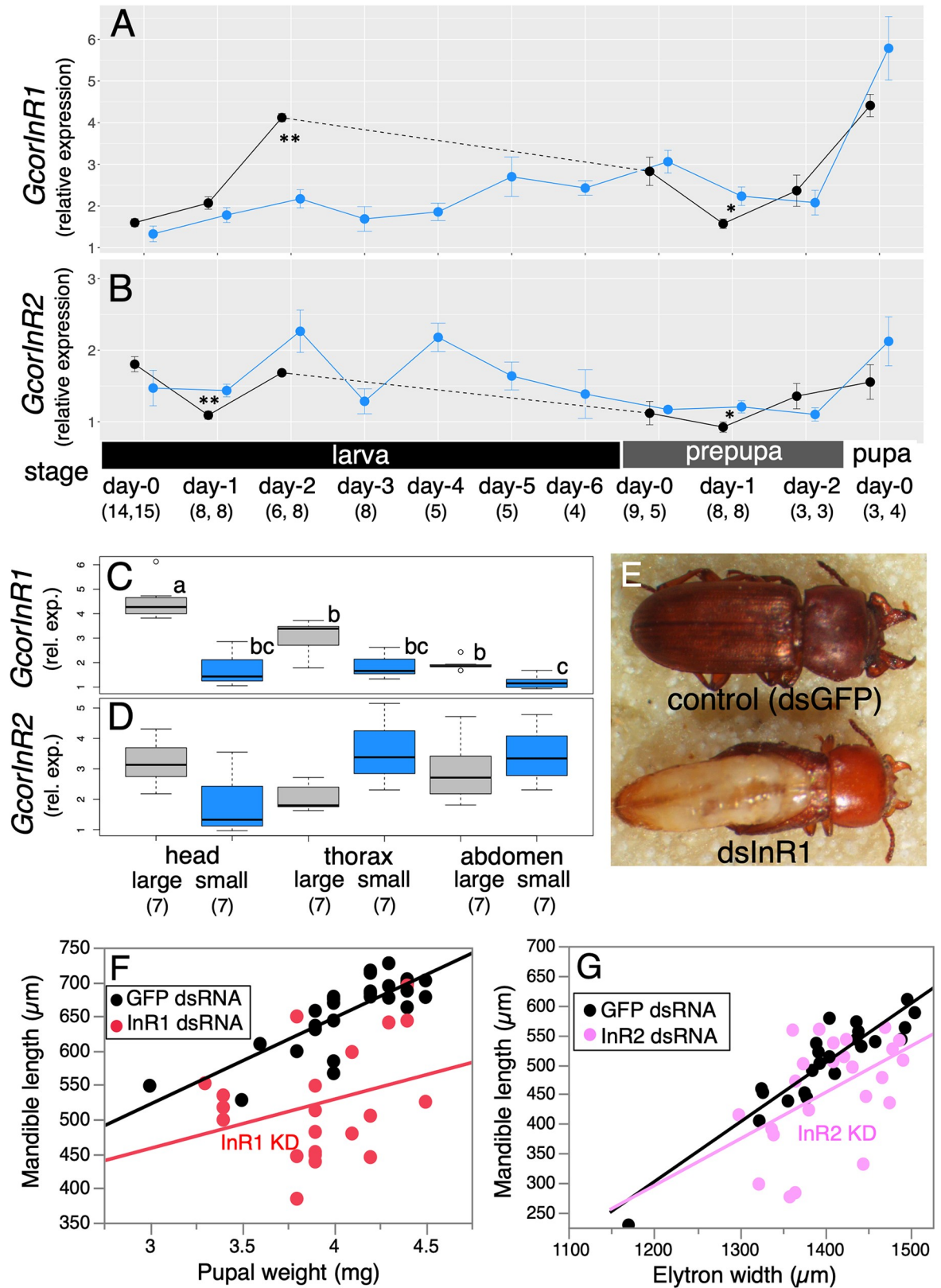


Fig 6. Functional analysis of insulin-like receptors. (A,B) *GcorInR1* and *GcorInR2* developmental dynamics, black: large larvae, blue: small larvae. Results are presented as mean \pm SE. Asterisks show significant differences between large and small larvae of the same stages

(Mann-Whitney U test, * $p < 0.05$, ** $p < 0.01$, *** $p < 0.001$). See Fig 3 caption for abbreviations day-0, -1, etc. (C,D) Body-part specificities of *GcorInR1* and *GcorInR2*. Different letters indicate significant differences (Steel-Dwass test). Gray: large, blue: small. Day-2 larvae were subjected to analysis. Gene expression levels relative to *Gcorgapdh* were quantified by qPCR. (E) *GcorInR1*^{RNAi} individuals suffered from severe systemic defects characterized by the malformation of fore- and hind wings, even under the weakest KD (28% reduction, S1 Table). (F) Mandible lengths were plotted against pupal weights for teratogenic *GcorInR1*^{RNAi} males and normal dsGFP males ($n = 21$ and 29 , respectively). (G) *GcorInR2*^{RNAi} males exhibited smaller mandible size without teratogenesis ($n = 24$ each) under intermediate level of KD (36% reduction, S1 Table). The underlying data in this figure are available from figshare (DOI: [10.6084/m9.figshare.9734780](https://doi.org/10.6084/m9.figshare.9734780); <https://figshare.com/s/609486022a3df39169bf>). dsGFP, double-stranded RNA for GFP; dsRNA, double-stranded RNA; *Gcorgapdh*, *G. cornutus* glyceraldehyde 3-phosphate dehydrogenase; *GcorInR*, *G. cornutus* InR; GFP, green fluorescent protein; InR, insulin-like receptor; KD, knockdown; qPCR, quantitative PCR; rel. exp., relative expression; RNAi, RNA interference.

<https://doi.org/10.1371/journal.pbio.3000541.g006>

These results strongly suggest that *GcorILP2* is the major molecular nature that facilitates conditional growth of the weapon. Generally, KD of *GcorILPs* did not affect survival from larva to adult, and the eclosed adults exhibited seemingly normal phenotypes.

GcorInR1 and GcorInR2 have functional redundancy for weapon morphogenesis

Next, we focused on the expression patterns and functions of two *GcorInRs* during development. The quantification of whole-body transcript levels from larva to pupa revealed that large individuals showed increased levels of *GcorInR1* during the larval stage (i.e., day-2 larvae), whereas these differences were diminished in prepupa day-0 and later stages (Fig 6A). *GcorInR2* expression showed no clear positive nutritional response during development (Fig 6A).

We further determined whether the expressions of two *GcorInRs* are body part specific, using the head, thorax, and abdomen of day-2 larvae. It is important to note that the head sample included mandible primordia and that the head itself exhibits positive allometry against body size [38,47]. We found that *GcorInR1* was highly expressed in the head of the large larvae (Fig 6C). Heightened expression of *GcorInR1* was also observed in the thorax of large larvae, but it was not significant in the abdomen (Fig 6C). *GcorInR2* was ubiquitously expressed across body parts (Fig 6D). Therefore, conditional expression of *GcorInR2* was unclear, although large larvae tended to express higher levels of *GcorInR2* in the head but nonsignificantly (Fig 6D).

Unlike *GcorILPs*, gene KD of *GcorInR1* was highly lethal before pupation. Even the smallest-dosage treatments (0.1 ng dsRNA, 28% reduction, S1 Table) caused the teratogenesis of adult posterior body and the failure of eclosion (see Fig 6E). This result is consistent with previous observations in *Drosophila* and *Tribolium* that *InR* mutant or KD phenotype showed severe defects in body growth and development [41,48]. Therefore, for *GcorInR1*^{RNAi} males, we used the pupal weight as an index of body size, and only adult mandibles were measured. *GcorInR1*^{RNAi} males exhibited a significant reduction of intercept (Fig 6F, ANCOVA, effect of treatment, $F = 49.5$, $p < 0.001$, see S2 Table for full model statistics). In contrast to *GcorInR1*^{RNAi} beetles, *GcorInR2*^{RNAi} beetles successfully eclosed under intermediate levels of KD (1 ng dsRNA, 36% reduction, S1 Table). In *GcorInR2*^{RNAi} males, there also was a significant decrease in mandible length as an intercept reduction (Fig 6G, ANCOVA, treatment, $F = 8.43$, $p = 0.034$, Bonferroni correction, see S2 Table for full model). Therefore, these two receptors likely have redundant functions in weapon growth. However, *GcorInR1* is more fundamental to systemic development, whereas *GcorInR2* is functionally more specific to mandible growth.

To quantify the changes in other traits, we firstly assessed the degree of trait size changes against dsGFP control in all treatments (S3 Table). Measurable *GcorInR1*^{RNAi} adults were not obtained; thus, they were excluded from the analysis. In *GcorILP2*^{RNAi} males, mandible length and width were greatly reduced (38%–55%); horn, head, and prothoracic sizes were moderately reduced (9%–25%); and elytra size was more consistent across treatments (2%–4%), indicating

that *GcorILP2* KD predominantly affects the mandibles but also reduces the anterior body size. Secondly, the change in overall phenotype was assessed by principal component analysis (PCA) using nine body-part measurements (S6 Fig, factor loadings in S4 Table). The lowered PC1 score of *GcorILP2^{RNAi}* males reflects the size reduction in anterior body parts. The lowered PC2 scores of *GcorILP2^{RNAi}* and *GcorInR2^{RNAi}* males indicated that KDs of these two genes yielded phenocopies similar in shape (i.e., relatively small anterior parts with larger posterior parts).

Taken together, these results strongly suggest that the fat body–derived *GcorILP2* regulates nutrient-dependent weapon growth through two functionally redundant *GcorInRs*, one of which (*GcorInR2*) has partially gained a weapon-specific morphogenetic function in *G. cornutus*.

Discussion

Specific ILP mediates conditional growth of weapon

Our study revealed that one specific type of ILP, *GcorILP2*, positively correlated with nutritional condition and had a specific function in weapon growth. Interestingly, size-dependent mandible growth was diminished, and mandible length was nearly maintained at the smallest size under KD of *ILP2*. These results strongly support that *ILP2* relays the nutritional condition to weapon growth in *G. cornutus*. So far, IIS has been proposed as the mechanism mediating conditional growth by receptor KD in horned beetles [10,12]. However, the exact ligand molecule that directly correlates with nutritional condition has not been identified in relation to the insect weapon. Besides insects, a rare example is found in deer, in which IGF-1 acts as a condition-dependent signal to accelerate antler growth [49,50]. Since IGF-1 is predominantly synthesized in the vertebrate liver, it is interesting to note that the liver and fat body, the two functionally equivalent organs between vertebrates and insects, have similar endocrinological systems to couple internal conditions with exaggerated trait growth. To our knowledge, this is the first evidence in insects to specify the actual messenger of IIS that underpins the conditional expression of sexually selected exaggerated traits.

In addition to the predominant effect on the mandibles, *GcorILP2* KD moderately reduced the head and prothorax sizes (S3 Table, S4 Table, S6 Fig). Such correlated changes in mandible and mandible-supporting traits are consistent with the developmental integration of functionally related modules (i.e., supportive traits, [51–53]). Unexpectedly, although similarly sized postfeeding larvae were subjected to KD experiments, the anterior body parts of *GcorILP2^{RNAi}* males decreased in size without increasing the other measured traits (S3 Table). We speculate that adult internal structures (e.g., fat body) are increased in *GcorILP2^{RNAi}* males, but this should be tested in future studies. Additionally, although genetic variation was considered to be low in our *G. cornutus* stock (see Materials and Methods), it may still contain some genetic variation. Thus, more work is required to determine whether genetic variation may also contribute to variation on larval growth dynamics.

Diversification of insect ILPs and *GcorILP2* function

From previous studies on *Drosophila*, ILP-mediated organ growth during larval development is generally considered to be a two-step process. The nutritional state is mainly sensed by the fat body [54], which in turn remotely regulates DILP secretion from brain neurosecretory cells through humoral signals called fat body–derived signals [55,56]. DILPs secreted from brain neurosecretory cells in turn control nutrient-dependent systemic body growth and metabolism during larval development. However, our results imply that the fat body–derived *GcorILP2* is used as a direct signal for adult organ growth without intervening in the central neurosecretory regulation.

Given that holometabolous insect larvae accumulate lipid and protein in the fat body for metamorphic morphogenesis [57], it is reasonable to assume that the larval fat body harbors information of nutritional state. At the postfeeding metamorphic stage, condition-dependent synthesis of GcorILP2 occurs in the fat body (peaking in day-2 larvae; Fig 3B) to regulate adult mandible growth in broad-horned flour beetles. Therefore, we suggest that, unlike the aforementioned two-step process, *G. cornutus* has a simple but elaborate growth regulatory mechanism in which a specific type of fat body-derived ILP directly couples nutritional condition with weapon growth. Whether the homologous and/or fat body-derived ILP subtype is repeatedly deployed in the conditional growth of weapons in other beetles and insects that independently gain weapons is an especially intriguing evolutionary question for future studies.

Importantly, however, our current argument on insect ILPs is largely based on derived holometabolous insects, such as Diptera and Lepidoptera. Therefore, the generality of the aforementioned two-step process is still uncertain, and the evolutionary process of insect insulin signaling is open to debate.

Our findings reflect the functional diversification of ILPs in other insect species. For example, ovarian activity is specifically regulated by *A. aegypti* ILP3 (*AaILP3*) in a mosquito and *Ooceraea biroi* ILP2 (*ObILP2*) in a clonal ant [23,58]. In body growth and metabolism, *AaILP6* has a specific interactive function with serotonin signaling in the fat body [25]. Combined with these previous studies, our findings highlight that ILP diversification plays a fundamental role in the ecophysiological diversification of insects. However, future comparative physiological studies across taxa are essential to understand the evolution of insect IIS.

Implication for module-specific complex growth

By receptor KDs, *GcorInR1*^{RNAi} males suffered high lethality, whereas *GcorInR2*^{RNAi} males could survive to become normal adults, suggesting that *GcorInR1* plays highly pleiotropic roles in systemic development (Fig 6E). A similar deleterious effect of *InR1* KD was also reported in red flour beetles during metamorphosis [41]. In contrast, relatively strong silencing of *GcorInR2* (36%) yielded normal adults with reduced mandibles (Fig 6G, S6 Fig), implying that, although *GcorInR1* and *GcorInR2* are functionally redundant in mandible development, *GcorInR2* has a more specific effect on mandible growth.

We would expect that *InR* localization can explain weapon-specific growth patterns [59]; however, the localization of *GcorInR1* and *GcorInR2* was paradoxical. *GcorInR1*, which had systemic effects, was strongly expressed in the head, whereas *InR2*, which had a specific effect on the mandibles, was ubiquitously expressed in the whole body (Fig 6C and 6D). An additional analysis confirmed that KD efficiency of *GcorInR2* was similar across body parts (43%, 41%, and 48% for the head, thorax, and abdomen, respectively, S1 Table), although there was a slight interaction effect between body part and KD treatment (two-way ANOVA, body part \times treatment, $F = 3.58$, $p = 0.037$). Therefore, the module specificity of KD effect and localization of *GcorInR2* did not coincide, and the aforementioned receptor-localization hypothesis was only partly supported for *GcorInR1*. We consider that the pleiotropic negative effect of *GcorInR1* was avoided by its localized expression, whereas *GcorInR2* somehow gained a weapon-specific growth function.

Theories of evolutionary genetics propose that duplicated genes with functional redundancy often differentiate into a state in which one of them gains functional novelty (i.e., sub-functionalization to neofunctionalization) [36,37,60]. A recent study in a dung beetle proposed a potential interaction of *doublesex* (*dsx*, the regulator of sex differentiation) with *InR2* but not with *InR1*, implying the functional differentiation of the two *InRs* [12]. The partly overlapping but differentiated functions of the two *GcorInRs*, as well as the distinctive

weapon-specific function of *GcorILP2*, can be understood in such evolutionary process, i.e., the functional diversification following the gene duplication.

As for module-specific conditional growth, several other mechanisms have been proposed (e.g., FOXO [12,61,62]; HDAC [42]). Additionally, juvenile hormone (JH), the central regulator of insect metamorphosis, is another well-known factor that facilitates weapon growth in several species, including *G. cornutus* [53,63–65]. Interestingly, *GcorILP2* ortholog *TcILP2* expression is inducible by JH in adult red flour beetles [66]. Future research to elucidate the links between these molecular pathways, as well as the downstream action of IIS and combinatorial functions of different ILPs, is required to fully understand the mechanisms underlying the complex growth of secondary sexual traits.

In conclusion, our study illustrates that functionally diversified IIS genes underlie the evolution of complex growth regulation in exaggerated traits.

Materials and methods

Broad-horned flour beetle (*G. cornutus*)

The *G. cornutus* stock population originated from adults collected in Miyazaki City, Japan. They were reared in the National Food Research Institute, Japan, and Okayama University, Japan, for about 50 years [38]. Therefore, the genetic variation in the stock population may be low. The stock was maintained with wholemeal flour enriched with yeast. The stock populations were reared in plastic containers (diameter, 40 mm; height, 30 mm) in groups of approximately 200 larvae, and they were provided with sufficient culture medium (wholemeal enriched with brewer's yeast [EBIOS, Asahi Group Foods, Tokyo, Japan]) [67].

Developmental schedule and staging

Timing of pupation is determined through critical size and food availability in *G. cornutus*. Additionally, its pupation is inhibited by larval crowding to avoid being the victim of cannibalism during molting, as is generally the case for Tenebrionidae [67,68]. In our experiment, larvae aged from 30 to 60 days after hatching (approximately 2–6 mg in weight) were transferred from sufficiently fed culture conditions to unfed solitary conditions (individual wells in a 24-well plate, VTC-P24, VIOLAMO) (Fig 1) [68]. We set these criteria according to the previous description and preliminary experiment that showed that they take approximately 30 days to reach the smallest size and 60 days to reach the maximum size [39,69].

The isolation from the stock (i.e., isolation from high-density conditions and food) led them to pupate within about a week; therefore, the age at isolation approximates the size of the focal larva and, consequently, that of the developed adult in this species. In Tenebrionidae, the number of instars and developmental time can vary according to diet conditions [70]. In our procedure, the total amount of diet was experimentally manipulated by isolating the larvae from the stock at various sizes and timings. In this procedure, the larvae that were <2.5 mg frequently failed metamorphosis and eventually died; therefore, we considered 2.5 mg to be the smallest size that allowed them to survive and develop into adults (i.e., critical size). Using the median size of larvae capable of metamorphosis as a criterion (S1 Fig), the larvae weighing 2.5–4 mg were defined as “small individuals” with poor nutrition and those weighing >4 mg as “large individuals” with abundant nutrition. To detect the size difference, we used the largest larvae (>4.5 mg) for the large category when available (85% [44 of 52] of large individuals were >4.5 mg).

The larval stages were defined as the days after isolation (e.g., a larva aged 1 day after isolation is referred to as a day-1 larva). Prepupation was visually checked every 24 hours to detect their characteristic L-shaped posture [67] (Fig 1). After the isolation from the stock, large

larvae (>4 mg) soon proceeded to the prepupal stage (2–4 days, Fig 1, S1 Fig), whereas small larvae (<4 mg) took longer for prepupation (3–8 days).

Developmental dynamics and tissue specificities of insulin signaling genes

Transcript dynamics from larval to pupal stages were examined by qRT-PCR using the whole body. For whole-body samples, total RNA was extracted with TRIzol (Invitrogen), treated with DNase I (RNA aqueous Micro Kit, Ambion), and reverse transcribed following the manufacturer's protocols of the High capacity cDNA RT kit (Applied Biosystems). Kapa SYBR Fast qPCR kit (KAPA) and Thermal Cycler Dice Real Time System II (Takara) were used to conduct qPCR, with gene-specific primers (S3 Table), fast PCR protocols, and crossing-point method following the manufacturer's instructions (Takara). According to the preliminary experiment, *Gcorgapdh* was confirmed as an appropriate normalization gene and thus used as a control gene in qRT-PCR. Relative quantification with the standard curve method was applied. Note that large larvae take less developmental time for prepupation (Fig 1, S1 Fig), and therefore, day-3 to day-6 large larvae were not available (Figs 2 and 6, dashed line).

To analyze body-part specificities of transcripts (Fig 6C and 6D), day-2 larvae after isolation were dissected in ice-cold 1 × PBS buffer. Individual larvae were used as cDNA samples of the head, thorax, and abdomen ($n = 7$ individuals). For small tissues (Fig 4B, S5 Fig), eight individuals were lumped together to obtain brain, fat body, and gut cDNA samples, and this procedure was replicated 7–12 times. For these tissue samples, total RNA was extracted with RNA aqueous Micro Kit (Ambion) and subjected to qPCR as described above.

For larval sexing (Fig 4), dsx primers spanning the sex-specific splicing region were used (S5 Table). The cDNA of test larvae was subjected to PCR (Takara exTaq, 35 cycles, 94°C for 1 minute, 55°C for 30 seconds, and 72°C for 30 seconds). PCR products were subjected to agarose gel electrophoresis, and sex-specific fragment patterns were used for sexing [71]. Individuals used in this analysis (Fig 4) partly overlapped with those used in Fig 3 as day-2 larvae ($n = 14$).

KDs of insulin signaling genes

Fully grown final instar larvae (approximately 60 days after hatching) were randomly selected from the stock and subjected to the dsRNA injection using Nanoject II (Drummond Scientific) under CO₂ anesthesia, then kept individually in 24-well plates without food. When KD efficiency was too severe to kill the test larvae and/or yielded teratogenic adults unsuitable for morphological measurements, dsRNA dosages were gradually titrated down from 50 ng to 0.1 ng (50 ng, 10 ng, 1 ng, 0.2 ng, and 0.1 ng). Among these, we selected the highest doses that allowed normal adult emergence (S1 Table).

Obtained adults (randomly selected 23–24 males for all treatments) were measured using a dissection microscope (VHX-200; KEYENCE) for mandible length, mandible width, horn length, gena width (lateral head structure), frontal prothorax width, maximum prothorax width, prothorax length, elytron length, and elytron width, as in previously described methods [42]. Elytron width was used as the index of body size [42]. As a control treatment, dsGFP (1 ng) was injected and analyzed as above. Bonferroni correction was applied to control for the multiple comparisons against the control. KDs of some genes were deleterious, and normal adults were not available even at the lowest levels of KDs (0.1 ng of dsRNA). In these cases, pharate adults were measured, and pupal weight was used as the body size.

Identification and classification of ILPs and InRs

Using the four ILPs (*ILP1–4*) [28] and two putative ILP receptors from the red flour beetle (InR1 and InR2, Gene IDs: 661524 and 664271) as queries, *G. cornutus* ILP and InR candidates

were retrieved by local BLASTx against the larval transcriptome (e-value < 1 for ILPs, e-value < 0.0001 for InRs) [42], and then the reciprocal best BLAST hit was confirmed [72]. Obtained sequences were manually checked for their identities by constructing amino acid alignments and phylogeny as follows.

For the ILP protein tree, annotated ILPs in flour beetles ($n = 4$) were included in the analysis. For the InR protein tree, we additionally used three coleopteran and four noncoleopteran insects with genome or transcriptome information available and human InR and IGF1R (S4 Fig) for speculation of cross-species orthologies. The evolutionary history was inferred by the maximum-likelihood method with a JTT matrix-based model and evaluated by bootstrap analyses ($n = 1,000$) using MEGA7 [73]. Analytical details are provided in figure captions (S3 and S4 Figs).

Owing to the extraordinarily diverged amino acid sequences in ILPs [34], ILP amino acid sequences were manually aligned by focusing on domain structures and characteristic cysteine residues according to a previous study [18].

Statistical analysis

For gene expression across tissues, either a parametric (Tukey's HSD) or nonparametric (Steel-Dwass test) method was applied according to the assessment of data distribution (Shapiro-Wilk test, $p > 0.05$, and Levene's test, $p > 0.05$ for parametric test). For the comparison of KD and control phenotypes, we used ordinary least-square regression and ANCOVA to analyze the effect of gene KD on mandible length using elytra length as a covariate (mandible length = elytra length + KD treatment + elytra length \times KD treatment). When the interaction term (elytra length \times KD treatment) was not significant after Bonferroni correction, the interaction term was removed from the model. We used EW as an index of body size because EW was the most stable trait across treatments (S4 Table). The statistical analyses were performed by JMP11 (SAS Institute) and R 3.5.1. (R Core Team 2018).

Supporting information

S1 Table. dsRNA dosages and RNAi efficiencies. dsRNA, double-stranded RNA; RNAi, RNA interference.
(DOCX)

S2 Table. Effect of gene KD on mandible length. Mandible lengths of KD treatments were compared to dsGFP control by ANCOVA using body size as covariate. Statistically insignificant interaction terms ($p > 0.05$) were removed from the model. For *GcorILP1-5* KD and *GcorInR2* KD, elytra width was used as body size. Pupal body weight was used as body size for *GcorInR1* KD in which measurable adults did not eclose (also see Results). For multiple comparison of *GcorILP1-5* KD and *GcorInR2* KD to the control treatment, p -values were adjusted by Bonferroni correction. dsGFP, double-stranded RNA for green fluorescent protein; *GcorILP1-5*, *G. cornutus* insulin-like peptides 1–5; *GcorInR2*, *G. cornutus* insulin-like receptor 2; KD, knockdown.
(DOCX)

S3 Table. Effect of gene KD on absolute trait size. Mean \pm SE is shown (μm). Fold changes to dsGFP control in mean sizes were shown in parenthesis. Bold letters indicate statistically significant differences from the control (Dunnett's test, $p < 0.05$). Note that mandibular traits are greatly reduced, head and thoracic traits are moderately reduced, and elytron traits are consistent by *GcorILP2* KD. dsGFP, double-stranded RNA for green fluorescent protein; EL, elytra length; EW, elytra width; FPW, frontal prothorax width; *GcorILP2*, *G. cornutus* insulin-

like peptide 2; GW, gena width; HL, horn length; KD, knockdown; ML, mandible length; MPW, maximum prothorax width; MW, mandible width; PL, prothorax length.
(DOCX)

S4 Table. Factor loadings for principal component analysis.
(DOCX)

S5 Table. Primer sequences for dsRNA synthesis and qPCR. *primers for sexing. dsRNA, double-stranded RNA; qPCR, quantitative PCR.
(DOCX)

S1 Fig. Developmental schedule depends on larval body size. The smaller larvae took longer time for prepupation after isolation from stock culture (i.e., high density and abundant food). Male, $Y = -1.175X + 9.13$, $R^2 = 0.50$, $p < 0.001$. Female, $Y = -1.950X + 11.7$, $R^2 = 0.60$, $p < 0.001$ (regression analysis).
(DOCX)

S2 Fig. Predicted prepropeptide structures of insulin-like, IGF-like, and DILP7-like peptides in *G. cornutus*. Domain-based alignment of (A) insulin-like peptides, (B) IGF-like peptides, and (C) DILP7-like peptides from broad-horned flour beetle (*G. cornutus*), red flour beetle (*T. castaneum*), fruit fly (*D. melanogaster*), yellow fever mosquito (*A. aegypti*), and honey bee (*A. mellifera*). Representative ILPs of *D. melanogaster* (DILP2, -6, -7), *A. aegypti* (AegILP3, -5, -6), and *A. mellifera* (AmILP1, -2) were shown. Highly conserved amino acid residues between all ILPs are shown in red, and highly conserved amino acid residues between orthologous ILPs in *G. cornutus* and *T. castaneum* are shown in green. Color bars indicate the predicted domains in the precursor peptides: green, signal peptide; red, B-chain; yellow, C-peptide; blue, A-chain; gray, D-domain. Asterisks on the color bars below the alignment denote Cys residues, and paired triangles denote potential cleavage sites (dibasic amino acids). GcorILP1-4 showed orthologous relationship with TcILP1-4, whereas GcorILP5 has no clear ortholog in *T. castaneum*. A group of insulin-like peptides (A) shares the most common structural feature of the ILP family, and GcorILP1, -2, -5 are classified into this group. The common feature of this group is a conserved domain organization of their precursors, consisting of a signal peptide, with a B-chain, C-peptide, and A-chain. After cleavage of the signal peptide, the C-peptide is most likely removed to generate a mature heterodimeric peptide consisting of the A- and B-chains like vertebrate insulin. A group of IGF-like peptides (B) is characterized by a relatively shortened or truncated C-peptide like vertebrate IGFs, and GcorILP3 is classified into this group. GcorILP3 has an extended A peptide (D-domain) as seen in TcILP3 and AegILP6 [30], which are more like the vertebrate IGFs. The third group, DILP7-like peptides (C), is characterized by an unusually conserved sequence shared by several insects, and GcorILP4 is classified into this group. AegILP, *A. aegypti* ILP; AmILP, *A. mellifera* ILP; DILP, *Drosophila* ILP; GcorILP, *G. cornutus* ILP; IGF, insulin-like growth factor; ILP, insulin-like peptide; TcILP, *T. castaneum* ILP.
(DOCX)

S3 Fig. Insulin-like peptide phylogeny based on amino acid sequences. Four of five *GcorILP* sequences had close similarities with corresponding *TcasILPs*, suggesting the orthologous relationships of these four genes. Bootstrap values (%), $n = 1,000$, maximum likelihood) are shown on the branches. Partial deletion model (90%) with 84 positions were used in final dataset. *GcorILP*, *G. cornutus* insulin-like peptide; *TcasILP*, *T. castaneum* insulin-like peptide.
(DOCX)

S4 Fig. Protein phylogeny of insulin-like peptide and IGF receptors. There are two major two clades in coleopteran InRs (type 1 and type 2 InRs). Twenty amino acid sequences from

nine insect species and human were included in the analysis (abbreviations: first letter of genus and first three letters of species, *G. cornutus*, broad-horned flour beetle; *T. castaneum*, red flour beetle; *Leptinotarsa decemlineata*, Colorado potato beetle; *O. taurus*, dung beetle; *Nicrophorus vespilloides*, burying beetle; *Zootermopsis nevadensis*, dampwood termite; *A. mellifera*, honey bee; *D. melanogaster*, fruit fly; *Nilaparvata lugens*, brown planthopper; *Homo sapiens*, human). Bootstrap values (% , $n = 1,000$, maximum likelihood) are shown on the branches. Partial deletion model (90%) with 1,086 positions were used in final dataset. IGF, insulin-like growth factor; InR, insulin-like receptor.

(DOCX)

S5 Fig. Source of *GcorILP1-5* transcripts. *GcorILP1,4,5* were predominantly synthesized in brain. *GcorILP1* expression was more abundant in small larvae. *GcorILP3* was ubiquitously expressed across tissues. Different letters indicate significant differences (*GcorILP1,3,5*: Steel-Dwass test; *GcorILP4*: Tukey's HSD test). Gray: large, blue: small. Day-2 larvae were subjected to analysis. Gene expression levels relative to *Gcorgapdh* were quantified by qPCR. *GcorILP*, *G. cornutus* insulin-like peptide; *Gcorgapdh*, *G. cornutus* glyceraldehyde 3-phosphate dehydrogenase; qPCR, quantitative PCR.

(DOCX)

S6 Fig. Principal component analysis based on sizes of nine body parts. RNAi phenotypes were represented by PC1-PC2 plot. PC1 was a size component positively loaded by all traits, and PC2 was a shape component positively loaded by mandible length, mandible width, and horn length (see S2 Table for factor loadings). Reduced PC2 scores in $ILP2^{RNAi}$ and $InR2^{RNAi}$. *ILP2*, insulin-like peptide 2; *InR2*, insulin-like receptor 2; PC, principal component; RNAi, RNA interference.

(DOCX)

S1 Material. Nucleotide sequences of *GcorILPs* and *GcorInRs*. *GcorILP*, *G. cornutus* insulin-like peptide; *GcorInR*, *G. cornutus* insulin-like receptor.

(DOCX)

Acknowledgments

We thank Drs. K. Kikue, T. Ozawa, T. Niimi, N. Posnien, and K. Ohta and the members of the Animal Ecology Lab. in TMU and M. Shimada Lab. in UT for invaluable feedback throughout the study. This work was supported by bioinformatic resources in NIBB and NIG.

Author Contributions

Conceptualization: Yasukazu Okada, Kensuke Okada.

Data curation: Yasukazu Okada, Masako Katsuki, Naoki Okamoto, Haruna Fujioka, Kensuke Okada.

Formal analysis: Yasukazu Okada, Masako Katsuki, Naoki Okamoto, Haruna Fujioka, Kensuke Okada.

Funding acquisition: Yasukazu Okada.

Investigation: Yasukazu Okada, Naoki Okamoto.

Methodology: Yasukazu Okada, Masako Katsuki, Naoki Okamoto.

Project administration: Yasukazu Okada.

Software: Haruna Fujioka.

Validation: Yasukazu Okada, Masako Katsuki, Kensuke Okada.

Visualization: Yasukazu Okada, Haruna Fujioka.

Writing – original draft: Yasukazu Okada, Masako Katsuki, Naoki Okamoto, Haruna Fujioka, Kensuke Okada.

Writing – review & editing: Yasukazu Okada, Naoki Okamoto, Kensuke Okada.

References

1. Andersson MB. Sexual selection. Princeton: Princeton University Press; 1994.
2. Gross MR. Alternative reproductive strategies and tactics: diversity within sexes. *Trends Ecol Evol.* 1996; 11: 92–98. [https://doi.org/10.1016/0169-5347\(96\)81050-0](https://doi.org/10.1016/0169-5347(96)81050-0) PMID: 21237769
3. Emlen DJ. Alternative reproductive tactics and male-dimorphism in the horned beetle *Onthophagus acuminatus* (Coleoptera: Scarabaeidae). *Behav Ecol Sociobiol.* 1997; 41: 335–341. <https://doi.org/10.1007/s002650050393>
4. Okada K, Miyatake T, Nomura Y, Kuroda K. Fighting, dispersing, and sneaking: Body-size dependent mating tactics by male *Librodor japonicus* beetles. *Ecol Entomol.* 2008; 33: 269–275. <https://doi.org/10.1111/j.1365-2311.2007.00965.x>
5. Huxley JS. Problems of relative growth. London: Methuen; 1932.
6. Shingleton AW, Frankino WA. New perspectives on the evolution of exaggerated traits. *BioEssays.* 2013; 35: 100–107. <https://doi.org/10.1002/bies.201200139> PMID: 23255216
7. Pigliucci M, Preston K. Phenotypic integration: studying the ecology and evolution of complex phenotypes. New York: Oxford University Press; 2004.
8. Gilbert SF, Epel D. Ecological developmental biology: integrating epigenetics, medicine, and evolution. Sunderland, MA: Sinauer Associates; 2009.
9. Lavine L, Gotoh H, Brent CS, Dworkin I, Emlen DJ. Exaggerated Trait Growth in Insects. *Annu Rev Entomol.* 2015; 60: 453–472. <https://doi.org/10.1146/annurev-ento-010814-021045> PMID: 25341090
10. Emlen DJ, Warren IA, Johns A, Dworkin I, Lavine LC. A mechanism of extreme growth and reliable signaling in sexually selected ornaments and weapons. *Science.* 2012; 337: 860–864. <https://doi.org/10.1126/science.1224286> PMID: 22837386
11. Koyama T, Mendes CC, Mirth CK. Mechanisms regulating nutrition-dependent developmental plasticity through organ-specific effects in insects. *Front Physiol.* 2013; 4 SEP: 1–12. <https://doi.org/10.3389/fphys.2013.00001>
12. Casasa S, Moczek AP. Insulin signalling's role in mediating tissue-specific nutritional plasticity and robustness in the horn-polyphenic beetle *Onthophagus taurus*. *Proc R Soc B Biol Sci.* 2018; 285. <https://doi.org/10.1098/rspb.2018.1631> PMID: 30963895
13. Nakae J, Kido Y, Accili D. Distinct and overlapping functions of insulin and IGF-I receptors. *Endocr Rev.* 2001; 22: 818–835. <https://doi.org/10.1210/edrv.22.6.0452> PMID: 11739335
14. Antonova Y, Arik AJ, Moore W, Riehle MA, Brown MR. 2—Insulin-Like Peptides: Structure, Signaling, and Function. In: Gilbert LIBT-IE, editor. San Diego: Academic Press; 2012. p. 63–92. Available from: <https://doi.org/10.1016/B978-0-12-384749-2.10002-0>
15. Nässel DR, Broeck J Vanden. Insulin/IGF signaling in *Drosophila* and other insects: Factors that regulate production, release and post-release action of the insulin-like peptides. *Cell Mol Life Sci.* 2016; 73: 271–290. <https://doi.org/10.1007/s00018-015-2063-3> PMID: 26472340
16. Thissen J-P, Ketelslegers J-M, Underwood LE. Nutritional Regulation of the Insulin-Like Growth Factors. *Endocr Rev.* 1994; 15: 80–101. Available from: <https://doi.org/10.1210/edrv-15-1-80> PMID: 8156941
17. Taguchi A, White MF. Insulin-Like Signaling, Nutrient Homeostasis, and Life Span. *Annu Rev Physiol.* 2008; 70: 191–212. <https://doi.org/10.1146/annurev.physiol.70.113006.100533> PMID: 17988211
18. Okamoto N, Yamanaka N. Nutrition-dependent control of insect development by insulin-like peptides. *Curr Opin Insect Sci.* 2015; 11: 21–30. <https://doi.org/10.1016/j.cois.2015.08.001> PMID: 26664828
19. Stewart CE, Rotwein P. Growth, differentiation, and survival: multiple physiological functions for insulin-like growth factors. *Physiol Rev.* 1996; 76: 1005–1026. <https://doi.org/10.1152/physrev.1996.76.4.1005> PMID: 8874492

20. Saltiel AR, Kahn CR. Insulin signalling and the regulation of glucose and lipid metabolism. *Nature*. 2001; 414: 799–806. <https://doi.org/10.1038/414799a> PMID: 11742412
21. Kremer LPM, Korb J, Bornberg-Bauer E. Reconstructed evolution of insulin receptors in insects reveals duplications in early insects and cockroaches. *J Exp Zool Part B Mol Dev Evol*. 2018; 2: 1–7. <https://doi.org/10.1002/jez.b.22809> PMID: 29888542
22. Xu HJ, Xue J, Lu B, Zhang XC, Zhuo JC, He SF, et al. Two insulin receptors determine alternative wing morphs in planthoppers. *Nature*. 2015; 519: 464–467. <https://doi.org/10.1038/nature14286> PMID: 25799997
23. Brown MR, Clark KD, Gulia M, Zhao Z, Garczynski SF, Crim JW, et al. An insulin-like peptide regulates egg maturation and metabolism in the mosquito *Aedes aegypti*. *Proc Natl Acad Sci*. 2008; 105: 5716–5721. <https://doi.org/10.1073/pnas.0800478105> PMID: 18391205
24. Chandra V, Fetter-Pruneda I, Oxley PR, Ritger AL, McKenzie SK, Libbrecht R, et al. Social regulation of insulin signaling and the evolution of eusociality in ants. *Science*. 2018; 361: 398–402. <https://doi.org/10.1126/science.aar5723> PMID: 30049879
25. Ling L, Raikhel AS. Serotonin signaling regulates insulin-like peptides for growth, reproduction, and metabolism in the disease vector *Aedes aegypti*. *Proc Natl Acad Sci*. 2018; 115: E9822–E9831. <https://doi.org/10.1073/pnas.1808243115> PMID: 30275337
26. Valzania L, Mattee MT, Strand MR, Brown MR. Blood feeding activates the vitellogenic stage of oogenesis in the mosquito *Aedes aegypti* through inhibition of glycogen synthase kinase 3 by the insulin and TOR pathways. *Dev Biol*. 2019; 454(1):85–95. Available from: <https://doi.org/10.1016/j.ydbio.2019.05.011> PMID: 31153832
27. Veenstra JA. The contribution of the genomes of a termite and a locust to our understanding of insect neuropeptides and neurohormones. *Front Physiol*. 2014; 5: 1–22. <https://doi.org/10.3389/fphys.2014.00001>
28. Li B, Predel R, Neupert S, Hauser F, Tanaka Y, Cazzamali G, et al. Genomics, transcriptomics, and peptidomics of neuropeptides and protein hormones in the red flour beetle *Tribolium castaneum*. *Genome Res*. 2008; 113–122. <https://doi.org/10.1101/gr.6714008> PMID: 18025266
29. Nässel DR, Liu Y, Luo J. Insulin/IGF signaling and its regulation in *Drosophila*. *Gen Comp Endocrinol*. 2015; 221: 255–266. <https://doi.org/10.1016/j.ygcen.2014.11.021> PMID: 25616197
30. Riehle MA, Fan Y, Cao C, Brown MR. Molecular characterization of insulin-like peptides in the yellow fever mosquito, *Aedes aegypti*: Expression, cellular localization, and phylogeny. *Peptides*. 2006; 27: 2547–2560. Available from: <https://doi.org/10.1016/j.peptides.2006.07.016> PMID: 16934367
31. Guo SS, Zhang M, Liu TX. Insulin-related peptide 5 is involved in regulating embryo development and biochemical composition in pea aphid with wing polyphenism. *Front Physiol*. 2016; 7: 1–12. <https://doi.org/10.3389/fphys.2016.00001>
32. Mizoguchi A, Okamoto N. Insulin-like and IGF-like peptides in the silkworm *Bombyx mori*: Discovery, structure, secretion, and function. *Front Physiol*. 2013; 4:217. <https://doi.org/10.3389/fphys.2013.00217> PMID: 23966952
33. Okamoto N, Yamanaka N, Satake H, Saegusa H, Kataoka H, Mizoguchi A. An ecdysteroid-inducible insulin-like growth factor-like peptide regulates adult development of the silkworm *Bombyx mori*. *FEBS J*. 2009; 276: 1221–1232. <https://doi.org/10.1111/j.1742-4658.2008.06859.x> PMID: 19175674
34. Okamoto N, Yamanaka N, Yagi Y, Nishida Y, Kataoka H, O'Connor MB, et al. A Fat Body-Derived IGF-like Peptide Regulates Postfeeding Growth in *Drosophila*. *Dev Cell*. 2009; 17: 885–891. <https://doi.org/10.1016/j.devcel.2009.10.008> PMID: 20059957
35. Slaidina M, Delanoue R, Gronke S, Partridge L, Léopold P. A *Drosophila* Insulin-like Peptide Promotes Growth during Nonfeeding States. *Dev Cell*. 2009; 17: 874–884. <https://doi.org/10.1016/j.devcel.2009.10.009> PMID: 20059956
36. Carroll S, Grenier J, Weatherbee S. From DNA to diversity: molecular genetics and the evolution of animal design. Wiley; 2004.
37. Ohno S, Wolf U, Atkin NB. Evolution from fish to mammals by gene duplication. *Hereditas*. 1968; 59: 169–187. <https://doi.org/10.1111/j.1601-5223.1968.tb02169.x> PMID: 5662632
38. Okada K, Miyanosita A, Miyatake T. Intra-sexual dimorphism in male mandibles and male aggressive behavior in the broad-horned flour beetle *Gnathocerus cornutus* (Coleoptera: Tenebrionidae). *J Insect Behav*. 2006; 19: 457–467. <https://doi.org/10.1007/s10905-006-9038-z>
39. Katsuki M, Okada Y, Okada K. Impacts of diet quality on life-history and reproductive traits in male and female armed beetle, *Gnathocerus cornutus*. *Ecol Entomol*. 2012; 37: 463–470. <https://doi.org/10.1111/j.1365-2311.2012.01390.x>
40. Nijhout HF. Size Matters (but So Does Time), and It's OK to Be Different. *Developmental Cell*. 2008; 15 (4):491–492. <https://doi.org/10.1016/j.devcel.2008.09.014> PMID: 18854132

41. Sang M, Li C, Wu W, Li B. Identification and evolution of two insulin receptor genes involved in *Tribolium castaneum* development and reproduction. *Gene*. 2016; 585: 196–204. <https://doi.org/10.1016/j.gene.2016.02.034> PMID: 26923187
42. Ozawa T, Mizuhara T, Arata M, Shimada M, Niimi T, Okada K, et al. Histone deacetylases control module-specific phenotypic plasticity in beetle weapons. *Proc Natl Acad Sci*. 2016; 113: 15042–15047. <https://doi.org/10.1073/pnas.1615688114> PMID: 27956627
43. Grönke S, Partridge L. The functions of insulin-like peptides in insects. *IGFs: Local Repair and Survival Factors Throughout Life Span*. Berlin: Springer; 2010. p. 105–124.
44. Brogiolo W, Stocker H, Ikeya T, Rintelen F, Fernandez R, Hafen E. An evolutionarily conserved function of the *Drosophila* insulin receptor and insulin-like peptides in growth control. *Curr Biol*. 2001; 11: 213–221. [https://doi.org/10.1016/S0960-9822\(01\)00068-9](https://doi.org/10.1016/S0960-9822(01)00068-9) PMID: 11250149
45. Miguel-Aliaga I, Thor S, Gould AP. Postmitotic specification of *Drosophila* insulinergic neurons from pioneer neurons. *PLoS Biol*. 2008; 6: 0538–0551. <https://doi.org/10.1371/journal.pbio.0060058> PMID: 18336071
46. Yang C, Belawat P, Hafen E, Jan LY, Jan Y-N. *Drosophila* egg-laying site selection as a system to study simple decision-making processes. *Science*. 2008; 319: 1679–1683. <https://doi.org/10.1126/science.1151842> PMID: 18356529
47. Okada Y, Suzaki Y, Miyatake T, Okada K. Effect of weapon-supportive traits on fighting success in armed insects. *Anim Behav*. 2012; 83: 1001–1006. <https://doi.org/10.1016/j.anbehav.2012.01.021>
48. Chen C, Jack J, Garofalo RS. The *Drosophila* insulin receptor is required for normal growth. *Endocrinology*. 1996; 137: 846–856. <https://doi.org/10.1210/endo.137.3.8603594> PMID: 8603594
49. Suttie JM, Gluckman PD, Butler JH, Fennessy PF, Corson ID, Laas FJ. Insulin-like growth factor 1 (IGF-1) antler-stimulating hormone? *Endocrinology*. 1985; 116: 846–848. <https://doi.org/10.1210/endo-116-2-846> PMID: 3881250
50. Gu L, Mo E, Yang Z, Zhu X, Fang Z, Sun B, et al. Expression and localization of insulin-like growth factor-I in four parts of the red deer antler. *Growth Factors*. 2007; 25: 264–279. <https://doi.org/10.1080/08977190701773187> PMID: 18092234
51. Tomkins JL, Kotiaho JS, LeBas NR. Phenotypic plasticity in the developmental integration off morphological trade-offs and secondary sexual trait compensation. *Proc R Soc B Biol Sci*. 2005; 272: 543–551. <https://doi.org/10.1098/rspb.2004.2950> PMID: 15799950
52. Okada Y, Suzaki Y, Miyatake T, Okada K. Effect of weapon-supportive traits on fighting success in armed insects. *Anim Behav*. 2012; 83. <https://doi.org/10.1016/j.anbehav.2012.01.021>
53. Okada Y, Gotoh H, Miura T, Miyatake T, Okada K. Juvenile hormone mediates developmental integration between exaggerated traits and supportive traits in the horned flour beetle *Gnatocerus cornutus*. *Evol Dev*. 2012; 14: 363–371. <https://doi.org/10.1111/j.1525-142X.2012.00554.x> PMID: 22765207
54. Colombani J, Raisin S, Pantalacci S, Radimerski T, Montagne J, Léopold P. A nutrient sensor mechanism controls *Drosophila* growth. *Cell*. 2003; 114: 739–749. [https://doi.org/10.1016/S0092-8674\(03\)00713-x](https://doi.org/10.1016/S0092-8674(03)00713-x) PMID: 14505573
55. Géminard C, Rulifson EJ, Léopold P. Remote Control of Insulin Secretion by Fat Cells in *Drosophila*. *Cell Metab*. 2009; 10: 199–207. <https://doi.org/10.1016/j.cmet.2009.08.002> PMID: 19723496
56. Droujinine IA, Perrimon N. Interorgan Communication Pathways in Physiology: Focus on *Drosophila*. *Annu Rev Genet*. 2016; 50: 539–570. <https://doi.org/10.1146/annurev-genet-121415-122024> PMID: 27732790
57. Arrese EL, Soulages JL. Insect Fat Body: Energy, Metabolism, and Regulation. *Annu Rev Entomol*. 2010; 55: 207–225. <https://doi.org/10.1146/annurev-ento-112408-085356> PMID: 19725772
58. Chandra V, Fetter-Pruneda I, Oxley PR, Ritger AL, McKenzie SK, Libbrecht R, et al. Social regulation of insulin signaling and the evolution of eusociality in ants. *Science*. 2018; 361: 398–402. <https://doi.org/10.1126/science.aar5723> PMID: 30049879
59. Hattori A, Sugime Y, Sasa C, Miyakawa H, Ishikawa Y, Miyazaki S, et al. Soldier morphogenesis in the damp-wood termite is regulated by the insulin signaling pathway. *J Exp Zool Part B Mol Dev Evol*. 2013; 320: 295–306. <https://doi.org/10.1002/jez.b.22501> PMID: 23703784
60. Rastogi S, Liberles DA. Subfunctionalization of duplicated genes as a transition state to neofunctionalization. *BMC Evol Biol*. 2005; 5: 1–7. <https://doi.org/10.1186/1471-2148-5-1>
61. Snell-Rood EC, Moczek AP. Insulin signaling as a mechanism underlying developmental plasticity: The role of FOXO in a nutritional polyphenism. *PLoS ONE*. 2012; 7: 1–11. <https://doi.org/10.1371/journal.pone.0034857> PMID: 22514679
62. Tang HY, Smith-Caldas MSB, Driscoll MV, Salhadar S, Shingleton AW. FOXO regulates organ-specific phenotypic plasticity in *Drosophila*. *PLoS Genet*. 2011; 7. <https://doi.org/10.1371/journal.pgen.1002373> PMID: 22102829

63. Gotoh H, Cornette R, Koshikawa S, Okada Y, Lavine LC, Emlen DJ, et al. Juvenile hormone regulates extreme mandible growth in male stag beetles. *PLoS ONE*. 2011; 6: 1–5. <https://doi.org/10.1371/journal.pone.0021139> PMID: 21731659
64. Cornette R, Gotoh H, Koshikawa S, Miura T. Juvenile hormone titers and caste differentiation in the damp-wood termite *Hodotermopsis sjostedti* (Isoptera, Termopsidae). *J Insect Physiol*. 2008; 54: 922–930. <https://doi.org/10.1016/j.jinsphys.2008.04.017> PMID: 18541259
65. Emlen DJ, Nijhout HF. Hormonal control of male horn length dimorphism in the dung beetle *Onthophagus taurus* (Coleoptera: Scarabaeidae). *J Insect Physiol*. 1999; 45: 45–53. [https://doi.org/10.1016/s0022-1910\(98\)00096-1](https://doi.org/10.1016/s0022-1910(98)00096-1) PMID: 12770395
66. Sheng Z, Xu J, Bai H, Zhu F, Palli SR. Juvenile hormone regulates vitellogenin gene expression through insulin-like peptide signaling pathway in the red flour beetle, *Tribolium castaneum*. *J Biol Chem*. 2011; 286: 41924–41936. <https://doi.org/10.1074/jbc.M111.269845> PMID: 22002054
67. Ozawa T, Ohta K, Shimada M, Okada K, Okada Y. Environmental Factors Affecting Pupation Decision in the Horned Flour Beetle *Gnatocerus cornutus*. *Zoolog Sci*. 2015; 32: 183–187. <https://doi.org/10.2108/zs140203> PMID: 25826068
68. Tsuda Y, Yoshida T. Population biology of the broad-horned flour beetle, *Gnathocerus cornutus* (F.) II. Crowding effects of larvae on their survival and development. *Res Popul Ecol (Kyoto)*. 1985; 27: 77–85. <https://doi.org/10.1007/BF02515481>
69. Tsuda Y, Yoshida T. Population Biology of the Broad-Horned Flour Beetle, *Gnathocerus cornutus* (F.) (Coleoptera: Tenebrionidae): I. Life Table and Population Parameters. *Appl Entomol Zool*. 1984; 19: 129–131.
70. Morales-Ramos JA, Rojas MG, Shapiro-Ilan DI, Tedders WL. Developmental Plasticity in *Tenebrio molitor* (Coleoptera: Tenebrionidae): Analysis of Instar Variation in Number and Development Time under Different Diets. *J Entomol Sci*. 2016; 45: 75–90. <https://doi.org/10.18474/0749-8004-45.2.75>
71. Gotoh H, Ishiguro M, Nishikawa H, Morita S, Okada K, Miyatake T, et al. Molecular cloning and functional characterization of the sex-determination gene *doublesex* in the sexually dimorphic broad-horned beetle *Gnatocerus cornutus* (Coleoptera, Tenebrionidae). *Sci Rep*. 2016; 6: 1–10. <https://doi.org/10.1038/s41598-016-0001-8>
72. Rivera MC, Jain R, Moore JE, Lake JA. Genomic evidence for two functionally distinct gene classes. *Proc Natl Acad Sci*. 1998; 95: 6239–6244. <https://doi.org/10.1073/pnas.95.11.6239> PMID: 9600949
73. Kumar S, Stecher G, Tamura K. MEGA7: Molecular Evolutionary Genetics Analysis Version 7.0 for Bigger Datasets. *Mol Biol Evol*. 2016; 33: 1870–1874. <https://doi.org/10.1093/molbev/msw054> PMID: 27004904